Magnetic Ratchet

A. Auge[1,*], F. Wittbracht[1], A. Weddemann [1] and A. Hütten [1]
[1]Department of Physics, University of Bielefeld, Universitätsstr. 25, 33615 Bielefeld, Germany
[*]Corresponding author: aauge@physik.uni-bielefeld.de

Abstract: Transport phenomena in spatially periodic magnetic systems far from thermal equilibrium are considered. The emphasis is put on directed transport of magnetic beads in a so called magnetic ratchet (Brownian motor). An asymmetric magnetic potential and Brownian motion of magnetic beads are the basic concepts for a magnetic ratchet. The asymmetric magnetic potential is achieved by combining an external magnetic field with a spatially periodic array of conducting lines. In this work simulations are carried out to test and optimize this asymmetric potential. As simulation model the Smoluchowski equation with flux terms for the magnetic and gravitational force is used. Furthermore experiments are carried out to verify the simulation results. Possible applications like transport in microfluidic devices and separation of magnetic beads are discussed.

Keywords: ratchet, transport, magnetic separation

1 Introduction

Micro Total Analysis Systems (µTAS), also called "Lab on a Chip", have received a growing interest over the last few years [12][2]. The aim of such systems is to integrate all laboratory tasks on one microfluidic chip. This includes the sample preparation, sample injection, sample manipulation, reaction, separation and detection.
Magnetic materials have gained importance for sample manipulation, separation and detection [10]. Magnetic markers (beads or particles) are used as carriers for biologic materials in such systems. The manipulation of magnetic markers has been realized via time varying electro-magnetic fields of for example a sawtooth[14] gold structure. Separations of magnetic markers has been shown via H-shaped microfluidic channels and the use of magnetic fields[8]. The detection of the magnetic markers can be realized via TMR[15] and GMR[3] sensors.
A further approach, that can be used to transport and separate particles, is the ratchet phenomenon[11]. The ratchet is a transportation phenomenon in the presence of diffusion and some perturbation that drives the system out of equilibrium without introducing a priori an obvious bias into one or the other direction of motion. Ratchet models have been introduced with different driving forces (potentials) and mechanisms. Due to the large number of different mechanisms, the emphasis is laid here on the on-off ratchet scheme. The on-off ratchet employs a spatially asymmetric potential that is switched on and off as underlying mechanism. Different driving forces have been introduced to manipulate particles with the on-off ratchet. The first experimental realization of an on-off ratchets employed a dielectric ratchet potential[13]. A similar approach to [13] was used in [4] to separate particles.
So far a combination of an on-off ratchet and a magnetic potential has not been discussed in literature. Such a combination might be well suited for applications in µTAS like transportation and separation with the possibility of evaluation via magnetic sensors. In this work a magnetic on-off ratchet is developed for transportation and separation of magnetic markers in µTAS.

2 Theoretical background

2.1 Magnetic fields and interaction with magnetic moments

A conducting line with current density $\vec{j}$ produces a magnetic field $\vec{H}$. For an arbitrary formed current density distribution the magnetic field is given by the law of Biot-Savart:

$$\vec{H}(\vec{r_1}) = \frac{1}{4\pi} \int \frac{\vec{j}(\vec{r_2}) \times \vec{e_{12}}}{r_{12}^2} dV_2 \qquad (1)$$

The magnetic field, that is generated by a conducting line, interacts with magnetic moments like magnetic particles or beads. The resulting force of the magnetic field on a bead in a liquid is:

$$F = F_{\text{mag}} - F_{\text{stokes}} \quad (2)$$

$$m\frac{\partial^2 \vec{x}}{\partial t^2} = -\mu_0(\vec{m}\cdot\vec{\nabla})\vec{H} + 6\pi\eta r\vec{v} \quad (3)$$

which leads for small systems to the following velocity:

$$\vec{v}(t) = \left(\frac{\mu_0(\vec{m}\cdot\vec{\nabla})\vec{H}}{6\pi\eta r}\right) \quad (4)$$

2.2 Diffusion in a potential

The basic equation that is used to describe the behavior of beads in this work is the Smoluchowski equation:

$$\frac{\partial c(x,t)}{\partial t} = \underbrace{-D\Delta c(x,t)}_{\text{diffusion}} + \underbrace{\vec{\nabla}\left(\frac{\vec{\nabla}U(r,t)}{6\pi\eta r}c(x,t)\right)}_{\text{drift}}$$

where $c(x,t)$ is the concentration of beads, U is some sort of potential, D is the diffusion coefficient, η the viscosity and r the bead radius. The potential U consists of a gravitation potential and a magnetic potential.

2.3 On- Off ratchet

A ratchet specifies a mechanism that allows only one direction of motion. In the other direction a force blocks the movement. There are many different concepts of ratchets[11]. In this work the concept of an on-off ratchet is used, which is introduced below.
A directed motion of particles in an on-off ratchet mechanism can be achieved by Brownian motion combined with a spatially periodic asymmetric potential.

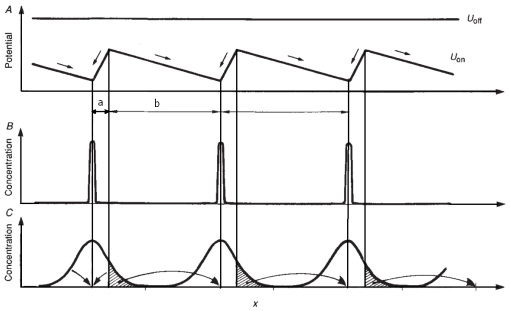

Figure 1: Schematic drawing of the principle of an on-off ratchet. Taken from [13]

In figure 1 the basic principle of an on-off ratchet is shown. The mechanism to induce directional motion is as follows. Suppose that the particles are on the bottom of the potential at the moment the potential is turned off (figure 1 B). During off states, the particle diffuses freely (figure 1 C). Because of the asymmetry of the potential, the distance to the maximum point of the potential on the steeper slope side is shorter than that on the gentler side. Thus the chance for the particle to go through the potential barrier on the steeper side (from now on called ratchet parameter a) is larger than that on the gentler side(from now on called ratchet parameter b). In figure 1 this situation is shown by the concentration distribution. The dashed area corresponds to the fraction of particles R_T, that diffused further than the distance a and hence is transported to the next potential minimum. Due to these different chances to reach a potential minimum, a net flux of particles arises.
The transport rate R_T can be calculated for a constant a and b via the following equation[1][6]:

$$R_T = \tfrac{1}{2}\cdot\left(\operatorname{erfc}\left(\frac{a}{\sqrt{4D\cdot(T_{\text{off}}-t)}}\right) - \operatorname{erfc}\left(\frac{b}{\sqrt{4D\cdot(T_{\text{off}}-t)}}\right)\right) \quad (5)$$

where $\operatorname{erfc}(x) = \frac{2}{\sqrt{\pi}}\int_x^\infty \exp(-t^2)dt$, T_{off} is the off- time of the potential and t a empirical latency time. The first term on the right hand side is the probability to diffuse further than a, while the second term takes account of back-diffusion, which is the probability to diffuse further than b. The macroscopic velocity of the particles can be calculated by the following equation[6]:

$$v = \frac{a+b}{T_{\text{on}}+T_{\text{off}}}R_T \quad (6)$$

where T_{on} is the on-time of the potential.

3 Geometry for a magnetic on-off ratchet

A possible geometry for a magnetic on-off ratchet is an assembly of spatially periodic conducting lines (shown in figure 1) in combination with a homogeneous external H_z-field.

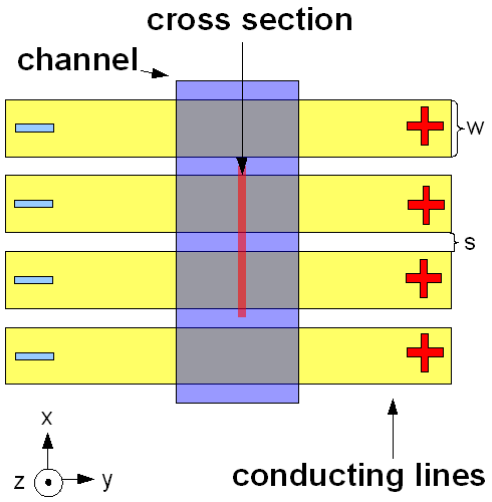

Figure 1: Sketch of the ratchet design

In this case the force on the beads changes to the following:

$$\vec{F}_{\text{mag}} = \begin{pmatrix} \mu_0 m_z \frac{\partial H_x}{\partial z} \\ \mu_0 m_z \frac{\partial H_z}{\partial z} \end{pmatrix} \tag{7}$$

F_{mag} leads to an asymmetric potential for the ratchet design, which is shown in figure 2.

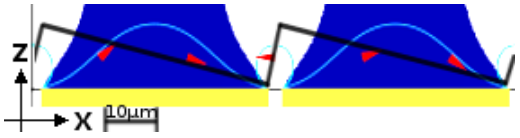

Figure 2: The area of the channel above the conducting lines is shown. In this area the force pointing to the right (left) is marked blue (white). The blue line corresponds to a magnetic field line. The black line shows a sketch of the potential, that marks the potential minimum and maximum for a bead directly above ground. The conducting line thickness is enlarged for a better overview. The arrows show $\vec{F}$.

The latter figure corresponds to a cross-section, which is marked in red in figure 1. For the simulation an Au conducting line with a width w of $40\mu m$, spacing of $3\mu m$ and a thickness of 100nm is assumed. The asymmetric potential directly above ground is highlighted by the black line. The force leading to this potential is colored as blue($+F_x$) and white ($-F_x$) areas.
To model the behavior of beads in the ratchet potential, the Smoluchowski equation is used.

$$\frac{\partial c}{\partial t} = \left(-D\Delta + \vec{\nabla} \left(\frac{\vec{F}_{\text{mag}} - Mg_z}{6\pi\eta r} \right) \right) c \tag{8}$$

where m_z the z-component of the magnetic moment of a bead, M the mass of a bead in water, H the magnetic field, c the concentration, g_z earth's standard surface gravity, η the viscosity and r the bead radius. Equation 8 is implemented using the weak formulation. To model the influence of bead- wall interaction in terms of height above ground z and bead radius r, the following two equations are used:

$$\lambda_{\parallel}(z) = 1 - \frac{9}{16}\left(\frac{r}{z}\right) + \frac{1}{8}\left(\frac{r}{z}\right)^3 - \frac{45}{256}\left(\frac{r}{z}\right)^4 - \frac{1}{16}\left(\frac{r}{z}\right)^5 + \ldots \tag{9}$$

$$\lambda_{\perp}^{-1} = 1 + \frac{9}{8}\left(\frac{r}{z}\right) \tag{10}$$

Equation 9 describes the influence on the horizontal component of diffusion and velocity [5] and equation 10 the influence on the vertical component, which is correct for $z \gg r$ [7]. Simulations employing equation 8 are used to determine the transport rate, the time T_{on} until all beads have moved to their potential minimum and the average height of beads. All values are found by integrating over the appropriate area and weighting the integrals with the according variables. For the average height, the area is the whole considered channel. The corresponding area for the on-time is the whole channel above one conducting line. For the transport rate, the area is given by the ratchet parameter a and back-diffusion. The transportation area is shown in figure 3 as yellow dashed area. The limit due to back-diffusion is shown by the green line. The end of the transportation area is the point where the two concentrations of two neighboring conducting lines meet. The ratchet parameter a is determined by the force components in F_x and F_z direction.

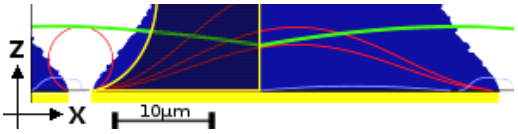

Figure 3: The area where the force points to the right is marked blue, the opposite direction is marked white. Trajectories of beads are plotted as red lines. The yellow dashed area is the part where beads get transported to the next potential minimum. The green line indicates the concentration after T_{off}=200s, while the blue line shows the concentration after the T_{on} time. The conducting line thickness is enlarged for a better overview.

The important line that determines the ratchet parameter a is the trajectory that ends at the channel lid in the area, where the force points to the right (colored in blue). Every bead that diffuses further than this line is transported to the next potential minimum. One important feature of this line, which also corresponds to the potential maximum, is the height dependence. Thus depending on the average height of a bead, the ratchet parameter a is different.

4 Experimental realization

4.1 Beads

There are two main requirements for magnetic beads. On the one hand magnetic beads have to have a high magnetic moment, on the other hand an agglomeration of magnetic beads is unwanted. These two requirements are well fulfilled by superparamagnetic beads. There are two kinds of beads used. To test the simulation model, MyOne beads from the company Invitrogen Dynal are used. These beads have a diameter of $1\mu m$ and a very small size distribution.
For separation measurements Chemagen M-PVA SAV1 beads from the company Chemagen are used due to their wide size distribution of 500nm-1.5μm.

4.2 Sample preparation

The magnetic ratchet is built in a two step lithography process. First, the parallel conducting lines are structured onto a native Si- Wafer via lift-off. For this process the positive photoresist AR-P5350 (Allresist GmbH, Gemany) is used. After spin-coating the resist for 30s at 4000rpm, the sample is heated to 85°C for 30 minutes. The lithography step itself is carried out with the DWL 66 (Heidelberg Instruments, Germany) laser lithography system. After development, 100nm holes are created via dry-etching in the UniLab (Roth&Rau,Germany). The holes are exactly filled with Au in a home-built sputter system. Next, a lift-off is carried out with the remover AR 300-70 (Allresist GmbH, Germany) in an ultrasonic bath.
In the second lithography step, the microchannel is structured onto the substrate. The negative resist SU-8 25 (Microchem, USA) is used as channel material. The resist is spinned onto the substrate for 30s at 2500rpm, which leads to channel height of $10\mu m$. Three baking steps are carried out. First, a soft-bake is applied (65°C for 5min, then 95°C for 15min). The sample is exposed with UV-light from a lithography system from Thermo Oriel. The exposure dose is 270mJ. Afterwards the post exposure bake (65°C for 5min, then 95°C for 5min) is applied. After developing the sample with SU-8 developer (Microchem, USA), the final hard bake (150°C for 15min) is performed. Afterwards the samples are wire bonded into dual-in-line IC-packages. After filling the channel with a bead solution, the microchannel is sealed with a PDMS lid. The PDMS lid is made with a Sylgard 184 elastomer kit.

4.3 Layout

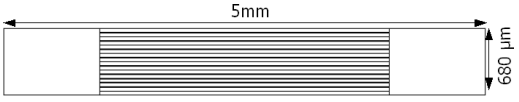

Figure 1: Layout for the experimental realization of the magnetic ratchet

For the experimental realization a layout with 16 parallel conducting lines is chosen with a width of $41\mu m$ and spacing of $2.5\mu m$. Here the situation of periodic boundary conditions is in good approximation fulfilled for the inner ten conducting lines. These inner ten conducting lines are used for experiments. The conducting lines are contacted with one bond on the left and right side.

4.4 Experimental setup

The experimental setup consists of an optical microscope with an attached CCD-camera and IC-socket that holds the sample. The microscope is an AXIOTECH VARIO carrying 4 EPIPLAN objectives (ZEISS, Germany) with magnification 5x, 20x, 50x, 100x and an 10x eyepiece. The self-made sample holder has an integrated IC-socket. All contacts of the IC-socket are connected to power supplies, measuring instruments and an analog-digital converter card in the computer. The CCD-camera M4+ CL (JAI, Japan) is mounted on top of the microscope and directly connected to a video grabber card in the computer. The current through a conducting line is measured and saved on the hard-disk together with the corresponding image and time. To ensure the absolute value of the magnetization to be comparable and the magnetization orientation of the magnetic beads to be perpendicular to the sample surface, a homogeneous magnetic field in z-direction is needed. This is achieved by usage of a self-made cylindrical coil that can be attached to the sample holder. For experiments a magnetic field of 500Oe is applied.

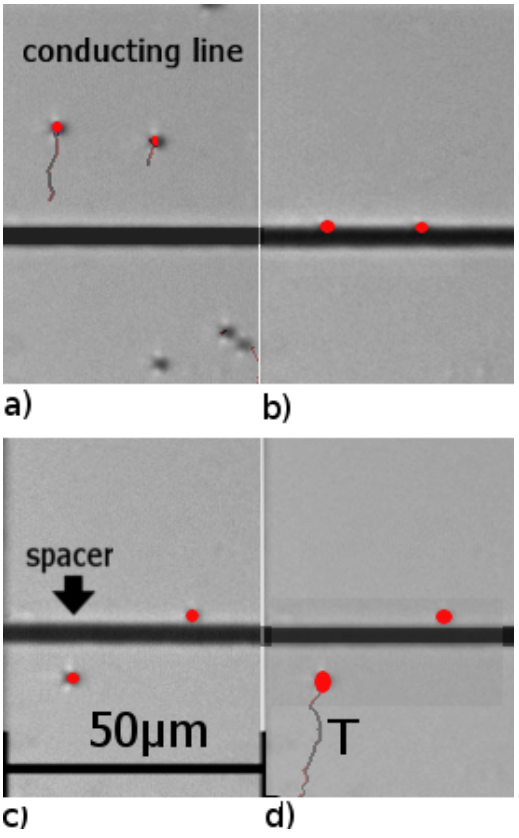

Figure 1: The magnetic ratchet shown in characteristic states. Beads discussed here are highlighted in red a) equilibrium state of the beads. The brown lines show part of the trajectory of the beads when the potential is switched on b) at the end of T_{on}. All beads that are not stuck to the ground have moved to the potential minimum c) off-state, beads start to diffuse freely. Here the situation after $T_{\text{off}} = 30s$ is shown d)The potential is switched on again after the time T_{off}. Beads that diffused further than the distance a are transported to the next potential minimum (marked with T)

5 Experimental Results

The evaluation of beads in the ratchet potential is done via video analysis. A detail of the typical observation area under the microscope ($330\mu m \times 330\mu m$) is shown as a picture sequence of the ratchet states in figure 1. Beads now discussed are highlighted in red. In the first picture a) the equilibrium state of beads is presented. The conducting lines appear as bright background, whereas the SiO_2 spacers appear as black line. Paths of two beads under the influence of the ratchet potential are shown. Tracking is achieved by using the tracking plugin MTRACK2 for ImageJ. The two beads move toward the lower end of the conducting line, which is shown in b). After the magnetic potential is switched off the beads start to diffuse freely. The situation after 30s is presented in c). Now the magnetic potential is switched on again.

While one bead is transported back to its origin, one bead gets transported to the next element (marked with T). This situation is presented in d). The trajectories show also the Brownian motion of the beads, which appears as a jerking movement which is superimposed by the directed movement in the potential. Video analysis allows to determine the transport rate and the T_{on} time to move all beads to their potential minimum.

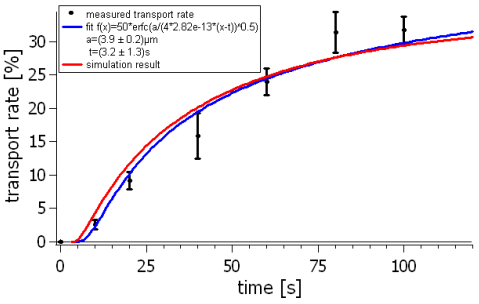

Figure 2: The measured transport rate as well as the simulation result is plotted. A fit to the measured transport rate data is done

In figure 2 the measured transport rate, the simulation result and a fit with equation 5 is shown. Each measured data point corresponds to the mean of at least 50 measurements. The experimental results for the transport rate fit well to the simulation result, if the latency time due to reduced diffusion at the ground and agglomeration effects is taken into account. The latency time is determined via the fitting parameter t of equation 5. The diffusion coefficient D for the fit has been experimentally determined via $\langle x^2 \rangle = 2Dt_{\text{diff}}$, where t_{diff} the diffusion time, and x the distance to the bead origin. The average T_{on} time to move all beads to their potential minimum with a current density of $4.8 \cdot 10^9 \frac{A}{m^2}$ in the conducting lines is $(14 \pm 2)s$. This time varies quite strongly since the trajectory of the beads depends on the initial conditions. Furthermore bead-bead interaction occurs, which can lead to attractive or repellent forces. Despite all above mentioned influences, the simulation result for the average time to move all beads to their potential minimum fits well to the measured value within the error. The highest macroscopic velocity is at T_{off}=25s. With this off-time, the average macroscopic velocity is about $(144 \pm 5)nm/s$.

5.1 Separation

Beads with different sizes show other macroscopic velocities in the magnetic ratchet. This size dependence can be utilized to separate beads according to size. For this, the difference in transport rates is used. The simulation result for the transport rates of 250nm, 500nm, and $1\mu m$ beads is shown in figure 3. For $1\mu m$ beads the measured latency time is used, while for the smaller beads a negligible latency time is expected [6].

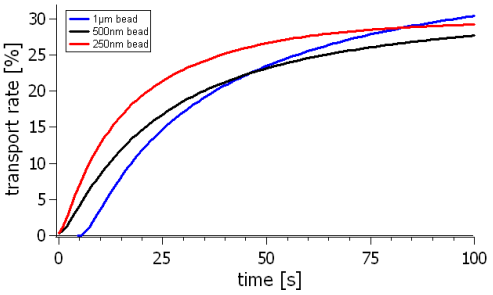

Figure 3: Transport rate for beads with a diameter of $1\mu m$ (blue line), 500nm(black line) and 250nm(red line) in dependence of the T_{off} time

One interesting feature of the transport rates is, that the transport rate for 500nm is not for all times higher as the one for $1\mu m$ beads. The reason for this is a different confinement and ratchet parameter a due to other average heights. For beads smaller than 500nm, in this example 250nm, the transport rate increases as expected with the diffusion constant D. Here the average height depends only on the channel height $(10\mu m)$ and not gravitation. To separate beads larger than $1\mu m$ from beads smaller than $1\mu m$, an off-time of 5s is chosen. Hence, beads larger than $1\mu m$ should not be transported to the next conducting line, while smaller ones should still be transported. A measurement of the transport rate proofs the simulation result. Beads smaller than $1\mu m$ show a transport rate of $R_T = (5.6 \pm 1.5)\%$, which fits within the error to the simulation result. With $T_{on} = (31 \pm 2)s$, which is the average time to transport all beads to their potential minimum, the average macroscopic velocity is $61 \pm 6nm/s$. Beads larger than $1\mu m$ have a transport rate of 0%. Hence with this ratchet design, it is possible to separate beads according to their size.

6 Discussion

We have introduced a magnetic ratchet that can be used for transportation as well as separation. Simulations and experimental results are in good agreement. The magnetic ratchet shows similar values for transportation ,separation times and sensitivity

as found in the literature [13] [4]. However, compared to other guided transport systems [16], where a macroscopic velocity of up to $200\mu m/s$ is achieved, the here achieved macroscopic velocity of 144nm/s is low. The basic limitation for the macroscopic velocity is the diffusion process. The separation process in the magnetic ratchet is slow compared to different methods. One popular method is continuous flow separation, where a throughput of 1.2mm/s is possible [9]. For the separation process an average macroscopic velocity of 60nm/s is achieved for beads smaller than $1\mu m$. However, one large advantage of the magnetic ratchet is, that no liquid motion and thus no micropumps are needed. To summarize, the magnetic ratchet might be applicable for transportation and separation in µTAS, if no large macroscopic velocities are required.

References

[1] A. Ajdari, J. Lewiner, J. Prost, and J. L. Viovy, *U.s. patent no. 5593565*, (1997).

[2] Pierre-Alain Auroux, Dimitri Iossifidis, Darwin R. Reyes, and Andreas Manz, *Micro total analysis systems. 2. analytical standard operations and applications*, Anal. Chem. **74** (2002), 2637–2652.

[3] R. L. Edelstein, C. R. Tamanaha, P. E. Sheehan, M. M. Miller, D. R. Baselt, L. J. Whitman, and R. J. Colton, *The barc biosensor applied to the detection of biological warfare agents*, Biosens. Bioelectron. **14** (2000), 805–813.

[4] L.P. Faucheux and A. Libchaber, *Selection of brownian particles*, J. Chem. Soc. Faraday Trans. **91** (1995), 3163.

[5] H. Faxen, Arkiv. Math. Astron. Fys. **17** (1923), 27.

[6] L. Gorre-Talini, S. Jeanjean, and P. Silberzan, *Sorting of brownian particles by the pulsed application of an asymmetric potential*, Phys. Rev. E **56** (1997), 2.

[7] H.A. Lorentz, Abhandl. Theoret. Phys. **1** (1906), 23.

[8] S. Ostergaard, G. Blankenstein, H. Dirac, and O. Leistiko, J. Magn. Magn. Mater **194** (1999), 156.

[9] N. Pamme, *Continuous flow separations in microfluidic devices*, Lab Chip **4** (2007), 1644–1659.

[10] Nicole Pamme, *Magnetism and microfluidics*, Lab Chip **6** (2006), 24–38.

[11] P.Reimann, *Brownian motors: noisy transport far from equilibrium*, Physics Reports **361** (2002), 57–265.

[12] Darwin R. Reyes, Dimitri Iossifidis, Pierre-Alain Auroux, and Andreas Manz, *Micro total analysis systems. 1. introduction, theory and technology*, Anal. Chem. **74** (2002), 2623–2636.

[13] Juliette Rousselet, Laurence Salome, Armand Ajdari, and Jacques Prost, *Directional motion of brownian particles induced by a periodic asymmetric potential*, Nature **370** (1994).

[14] R.Wirix-Speetjens and J. de Boeck, IEEE Trans.Magn. **40** (2004), 1944.

[15] Jrg Schotter, *Development of a magnetoresistive biosensor for the detection of biomolecules*, Ph.D. thesis, University of Bielefeld, 2004.

[16] Pietro Tierno, V. Reddy, Jing Yuan, Tom Johansen, and Thomas Fischer, *Transport of loaded and unloaded microcarriers in a colloidal magnetic shift register*, J. Phys. Chem. B **111** (2007), 13479–13482.